# Bound and continuum states of molecular anions C2H— and C3N—

**— Source link** ↗

Stephen Harrison, Jonathan Tennyson

**Topics:** Elastic scattering, Bound state, Excited state, Atomic orbital and Scattering

Related papers:

- Laboratory and Astronomical Detection of the Negative Molecular Ion C3N

- Detection of c5n and vibrationally excited c6h in irc +10216

- Laboratory and Astronomical Identification of the Negative Molecular Ion C6H

- Astronomical identification of CN - , the smallest observed molecular anion

- Astronomical detection of C$\mathsf{_{4}H^-}$, the second interstellar anion

# Bound and continuum states of molecular anions C2H and C3N

Stephen Harrison, Jonathan Tennyson

# Bound and continuum states of molecular anions $C_2H^-$ and $C_3N^-$

**Stephen Harrison and Jonathan Tennyson**

Department of Physics and Astronomy, University College London, Gower St.,
London WC1E 6BT, UK

**Abstract.**
   Recently a number of molecular anions, closed-shell linear carbon chains of the
form $C_nH^-$ and $C_nN^-$, have been detected in space. The molecules $C_2H^-$ and $C_3N^-$
are investigated by using the R-Matrix method to consider electron scattering from
the corresponding neutral targets. Initial target calculations are conducted and refined
in order to produce target state characteristics similar to the experimental data. A
number of different scattering models are tested including static exchange and close-
coupling models, and the use of Hartree-Fock or natural orbitals in the close-coupling
calculations. The calculations concentrate on bound and resonances states for the
anions as well as eigenphase sums, elastic cross-sections and electronic excitation cross-
sections for electron collisions with the neutral. It is found that electronic resonances
are all too high in energy to be important for anion formation in the interstellar
medium. However, $C_3N^-$, unlike $C_2H^-$, supports a number of very weakly bound
excited states, which may well provide the route to electron attachment for this system.

## 1. Introduction

The first anion detected in space was $C_6H^-$ by McCarthy et al. (2006). Since then $C_4H^-$
(Gupta et al. 2007), $C_8H^-$ (Brunken et al. 2007), $C_3N^-$ (Thaddeus et al. 2008) and $C_5N^-$
(Cernicharo et al. 2008) have also all been detected. $CN^-$, $C_3N^-$ or $C_4H^-$, and $C_5N^-$
have also recently been identified in the atmosphere of Titan (Vuitton et al. 2009). Since
the present work was completed, $CN^-$ has also been detected in the interstellar medium
(ISM) (Agundez et al. 2010). These anions are all linear multiply-bonded carbon chains
with closed shell ground state configurations. The prevailing opinion is that these anions
are formed by radiative attachment of an electron to the neutral molecule with the same
chemical formula (Millar et al. 2007). These neutral precursors are all linear multiply-
bonded carbon chains with significant dipole moments which are known to exist in the
interstellar medium. The corresponding anions are closed shell molecules whose extra
electron is bound by several eV.
   Herbst and co-workers (Petrie & Herbst 1997, Terzieva & Herbst 2000, Herbst &
Osamura 2008) developed and applied a model for calculating radiative association rates
for these $C_nH^-$ and $C_{n+1}N^-$ ($n$ even) species. This model is based on the formation
of low-lying resonances in electron collisions and fairly simple phase-space arguments.

Studies suggest that although this model gives anion formation rates of approximately the right magnitude, the rates it provides cannot actually reproduce the observations (Harada & Herbst 2008).

Although there have been a number of electronic structure studies of these anions (see for example Woon (1995), Natterer & Koch (1995), Botschwina & Oswald (2008), Fortenberry et al. (2010)), there appears to have been no previous study of their continuum states. We have therefore performed a series of studies of electron collisions with both $C_nH$ and $C_{n+1}N$ ($n$ even) targets. Initially our studies focussed on electron collisions with $C_4H$ and $C_3N$ as the first member of each series for which the associated anion had been observed in the interstellar medium. However we found it difficult to establish definitive properties for the ground state of $C_4H$, a problem that is well-documented (Fortenberry et al. 2010). Although we have performed a series of electron collision studies with $C_4H$, here we report electron collision calculations which focus on $C_2H$ and $C_3N$ as we consider the results of these calculations to be more reliable.

## 2. Method

Scattering calculations were performed using the R-matrix method (Burke & Berrington 1993), whose use for collision calculations involving molecules has recently been extensively reviewed by one of us (Tennyson 2010). The basic idea of the R-matrix method is the division of space into two regions: a spherical inner region of radius $a$ which is designed to enclose all the charge density of the target, and an outer region where interactions between the electron and the target can be represented by long-range moments. The major advantage of the method is that within the inner region the problem is solved independent of scattering energy. Within this region the wavefunction is written:

$$\psi_k^{N+1} = \mathcal{A} \sum_{ij} a_{ijk} \Phi_i^N(\mathbf{x}_1...\mathbf{x}_N) u_{ij}(\mathbf{x}_{N+1}) + \sum_i b_{ik} \chi_i^{N+1}(\mathbf{x}_1...\mathbf{x}_{N+1}), \quad (1)$$

where the target contains $N$ electrons and functions are labelled as $N$ or $N+1$ according to whether they refer to the target or the compound scattering system respectively. In this work all orbitals underlying the wave functions of eq. (1) were constructed from Gaussian Type Orbitals (GTOs); as discussed below a variety of different orbital sets (Hartree-Fock, CASSCF and Natural orbitals) were tested. In this regard one issue is the requirement to represent all target states included in the calculation with a single orbital set.

In eq. (1), $\Phi_i^N$ is the wave function of $i^{\text{th}}$ target state. $u_{ij}$ are the extra orbitals introduced to represent the scattering electron (Faure et al. 2002). The operator $\mathcal{A}$ ensures that the product of these two terms obeys the Pauli principle. The second summation in eq. (1) involves $L^2$ configurations which have no amplitude on the R-matrix boundary and where all electrons are placed in orbitals associated with the target. As we are dealing with electron collision with strongly dipolar systems, it is necessary to allow for the contribution of electron interactions with the long-range target

dipole moment to any cross sections calculated. This was carried out using the program BORNCROS (Baluja et al. 2000), which directly calculates the dipole Born correction to the cross-sections.

The scattering calculations reported here were performed using the UK molecular R-matrix codes (Morgan et al. 1998), mostly starting from the Quantemol-N interface (Tennyson et al. 2007). Target electronic structure calculations were largely performed with MOLPRO (Werner et al. 2008), which was also used to provide many of the sets of target molecular orbitals. For both molecules scattering calculations were performed at two levels: static exchange (SE), which is useful for identifying shape resonances, and close coupling (CC). The presence of very low-lying excited target states meant that the widely used one-state static exchange plus polarisation model was deemed inappropriate for this study, as this method is prone to giving pseudoresonances at energies above the first electronically excited target state.

All calculations were performed at the equilibrium geometry of the neutral target and ignored effects due to nuclear motion. We note that although all molecules considered here are linear, neither the polyatomic R-matrix codes nor MOLPRO use $C_{\infty v}$ symmetry. All calculations were therefore performed using $C_{2v}$ symmetry. In most cases identifying the results in $C_{\infty v}$ is straightforward and these symmetry labels are largely used below.

## 3. $C_2H^-$

In choosing appropriate target wavefunctions to include in the scattering calculation a number of criteria are used. Firstly, the target model must be one for which an appropriate, balanced scattering model can be designed (Tennyson 1996). For this a complete active space configuration interaction (CAS-CI) model is often adopted. Secondly the excitation energy of important target electronic states should be approximately correct. Thirdly other target properties, in particular for strongly polar molecules, the permanant dipole moment of the ground state, should be well represented. Satisfying all these criteria for the systems studied here proved to be difficult and led to some compromises being made. Indeed we note that for $C_4H^-$ electronic structure calculations performed without requirement to use the resulting wavefunction in a scattering calculation struggled to satisfy the other requirements (Fortenberry et al. 2010).

### 3.1. Target calculations

A variety of models were tested when calculating results for the neutral $C_2H$ target, a selection of these are shown in Table 1. Models 1 – 6 were carried out using the R-Matrix software Quantemol-N. These comprised Hartree-Fock (HF) and Complete Active Space Configuration-Interaction (CAS-CI) calculations using each of the 3 basis sets, DZP, cc-pVDZ and cc-pVTZ. The CAS-CI calculations used an orbital space of 7,2,2 orbitals of

**Table 1.** Selected calculated target properties of $C_2H$. All results are for the equilibrium geometry of $C_2H$. The calculated absolute energies of the X $^2\Sigma^+$ ground state is given in Hartree while the vertical excitation energy to the low-lying A $^2\Pi$ is given in eV. $\mu$ is the ground state dipole moment, given in Debye. See text for details of models.

| Model | Basis | Orbitals | Method | X $^2\Sigma^+$ | $\mu$ | A $^2\Pi$ |
|---|---|---|---|---|---|---|
| This work/1 | DZP | SCF | HF | -76.142 | 0.804 | 1.186 |
| 2 | DZP | SCF | CAS-CI | -76.200 | 0.837 | 1.204 |
| 3 | cc-pVDZ | SCF | HF | -76.138 | 0.789 | |
| 4 | cc-pVDZ | SCF | CAS-CI | -76.207 | 0.801 | 1.304 |
| 5 | cc-pVTZ | SCF | HF | -76.156 | 0.797 | |
| 6 | cc-pVTZ | SCF | CAS-CI | -76.208 | 0.801 | 1.248 |
| 7 | cc-pVTZ | NOs | CAS-CI | -76.296 | 0.640 | 1.089 |
| Woon (1995) | cc-pVDZ | | RCCSD(T) | -76.401 | 0.766 | 0.361 |
| | cc-pVTZ | | RCCSD(T) | -76.468 | 0.774 | 0.402 |
| | CBS limit | | RCCSD(T) | -76.499 | | 0.423 |
| Cui & Morokuma (1998) | cc-pVTZ | | CASPT2 | -76.458 | | 0.790 |

symmetry $a_1$, $b_1$, $b_2$ respectively which maps to 7 $\sigma$ and 2 $\pi$ orbitals. Eight electrons were frozen in the $1-4\sigma$ orbitals with five active electrons distributed amongst the $5-7\sigma$ and $1-2\pi$. Model 7 used this CAS-CI model but the molecular orbitals used in the calculation were produced by MOLPRO, in this case using a multireference CI (MRCI) calculation, and the R-Matrix calculation was carried out using the R-Matrix codes manually, to allow for use of MOLPRO orbitals. These natural orbitals (NOs) were state averaged from 3 states produced one each from $^2A_1$, $^2B_1$ and $^2B_2$, ($^2\Sigma^+$ and $^2\Pi$) MRCI calculations, using the MOLPRO 'MATROP' facility, with a 13:1:1 weighting. This weighting was chosen to create a target model with good characteristics for the scattering calcuation i.e. a good reproduction of the excitation energies and dipole moment in comparison with the orginal MOLPRO calculations. Use of the pure $^2A_1$ MRCI orbitals was found to make the first vertical excitation energy too high in energy by a factor of 2, and the use of more equally weighted state-averaged orbitals was found to reduce the dipole to a value too small to be acceptable in the scattering calculation by up to a factor of 3. Hence model 7 was deemed acceptable in describing both these characteristics without sacrificing one in favour of the other. Whilst we were able to find some experimental data for the bound state energy of the anion, we could not find any data on the neutral, such as the dipole moment.

There have been a number of previous *ab initio* studies on $C_2H$; Table 1 compares our models with the best of these. As we only use a very limited correlation space, the other studies give lower absolute energies even for calculations which use the same target basis. Our dipole moments are in reasonable agreement with those predicted by Woon (1995). However our predictions for the vertical energy of excitation for the very low-lying A $^2\Pi$ state appear to systematically to high.

**Table 2.** $C_2H^-$ bound states with energies given in eV. All calculations are for the equilibrium geometry of $C_2H$

| Model | Basis | Orbitals | Method | $^1\Sigma^+$ Binding energy (eV) |
|---|---|---|---|---|
| This work/1 | DZP | SCF | SE | 1.186 |
| 2 | DZP | SCF | CC | 2.713 |
| 3 | cc-pVDZ | SCF | SE | 1.114 |
| 4 | cc-pVDZ | SCF | CC | 2.637 |
| 5 | cc-pVTZ | SCF | SE | 1.156 |
| 6 | cc-pVTZ | SCF | CC | 2.617 |
| 7 | cc-pVTZ | NOs | CC | 2.282 |
| Baker et al. (1986) | 6-311$^{++}$G | UHF | UHF | 1.56 |
| | 6-311$^{++}$G | UHF | UCISD | 2.62 |
| Janousek et al. (1979) | | | experiment | 2.94±0.10 |
| Ervin & Lineberger (1991) | | | experiment | 2.969±0.006 |
| Taylor & Xu (1998) | | | experiment | 2.956±0.020 |

### 3.2. Scattering calculations and bound anion states

Our scattering calculations concentrated on finding bound states and resonances for $C_2H^-$ but also provide low-energy electron – $C_2H$ collision cross sections. Two classes of models were tested: SE based on a single target state and CC models where 48 state calculations (doublet and quartet states, 6 states per symmetry) were performed in the inner region. As discussed below, different numbers of these states were retained in the outer region of the calculation.

Bound states were calculated using the outer region program BOUND (Sarpal et al. 1991). For these calculations only the low-lying X $^2\Sigma^+$ and A $^2\Pi$ were retained in the outer region of the CC calculations, since experience has shown that strongly closed states can cause such outer region calculations to be numerically unstable. These were propagated to a distance of 30.1 $a_0$. Table 2 summarizes the results of these studies. In contrast to $C_3N^-$ discussed below, all models found only a single bound state. The SE calculations give a vertical binding energy of about 1.2 eV whereas for the CC calculations this binding energy is increased to about 2.6 eV. These figures are in broad agreement with the electronic structure calculations of Baker et al. (1986). The CC binding energies are some 0.6 eV less than the measured ones; however the measured binding energies are adiabatic and will therefore be higher than our calculated vertical ones.

### 3.3. Resonances

Outer region calculations were performed retaining those target states which lie below 10 eV for the CC calculations, the Quantemol-N default setting. This means 25 states for

**Table 3.** $C_2H^-$ low lying resonance positions (and widths) in eV

| Model | 1 | 2 | 3 | 4 | 5 | 6 | 7 |
|---|---|---|---|---|---|---|---|
| $^1\Sigma^+$ | | | | | | | 2.957 (0.122) |
| $^1\Sigma^-$ | | 3.876 (1.115) | | 4.231 (1.056) | | 3.908 (1.080) | 5.130 (1.596) |
| $^3\Sigma^+$ | | 2.589 (0.430) | | 2.768 (0.377) | | 2.679 (0.444) | 2.923 (0.127) |
| | | | | | | | 3.942 (0.125) |
| $^3\Pi$ | 3.522 (1.949) | 3.49 a | 3.634 (2.038) | 3.380 (1.360) | 3.562 (2.021) | 3.53 a | 3.682 (2.742) |
| $^3\Sigma^-$ | | 3.374 (0.867) | | 3.625 (0.814) | | 3.416 (0.854) | 4.495 (1.298) |

$^a$ Resonance present in eigenphases but not fitted by RESON.

models 2, 4 and 6 but only 16 for model 7. The results reported below are insensitive to increasing these numbers. Resonances were characterised using a Breit-Wigner fit to the eigenphases, which are shown in Figure 1, as implemented in the automated detection and fitting program RESON (Tennyson & Noble 1984). As noted below, resonances which overlap excitation thresholds were not fitted by this procedure. Only low-lying resonances were considered since higher resonances are unlikely to be important in any radiative association process.

Table 3 summarizes the resonances detected for $C_2H^-$. The SE calculations all detect a single shape resonance of $^3\Pi$ symmetry at about 3.5 eV. At the SE level this is a very broad resonance with a width of about 2 eV. In the CC calculations this resonance postition is lowered to about 3.4 eV and becomes considerably narrower with SCF orbitals and broader with MRCI NO's. The CC calculations based on the use of SCF orbitals introduce Feshbach resonances of $^1\Sigma^-$, $^3\Sigma^+$ and $^3\Sigma^-$ symmetry. Use of NOs introduce a further narrow $^3\Sigma^+$ resonance. We note that none of these resonances lie below the A $^2\Pi$ first excited state of $C_2H$.

### 3.4. Cross-sections

Figure 2 presents the total elastic cross-section of $C_2H$ for electron scattering energies up to 10 eV, for all 3 models, SCF-SE, SCF-CC and MRCI-CC. For the final MRCI-CC model, a Born correction was applied due to the dipolar nature of the molecule, which acts to increase the cross-section at all energies.

Electron impact electronic excitation cross sections are given by the many-state CC calculations. Figure 3 shows the cross-sections representing the excitation from the $^2\Sigma^+$ ground state of the neutral to the first three excited states, A $^2\Pi$, a $^4\Sigma^+$ and b $^4\Delta$. Here the Born correction is only applied to the $^2\Pi$ excitation, as this is the only dipole-allowed transition. All three excitation cross sections show resonance features. These are particularly pronounced in the CC-MRCI calculations; we note that cross sections approximately average the SCF-CC ones which show fewer resonances. Although it is likely that these cross sections display resonance features, they can only be properly characterised by much larger calculations than the one presented here.

### 4. $C_3N^-$

Calculations on $C_3N$ and $C_3N^-$ follow closely those on $C_2H$ and $C_2H^-$ reported above.
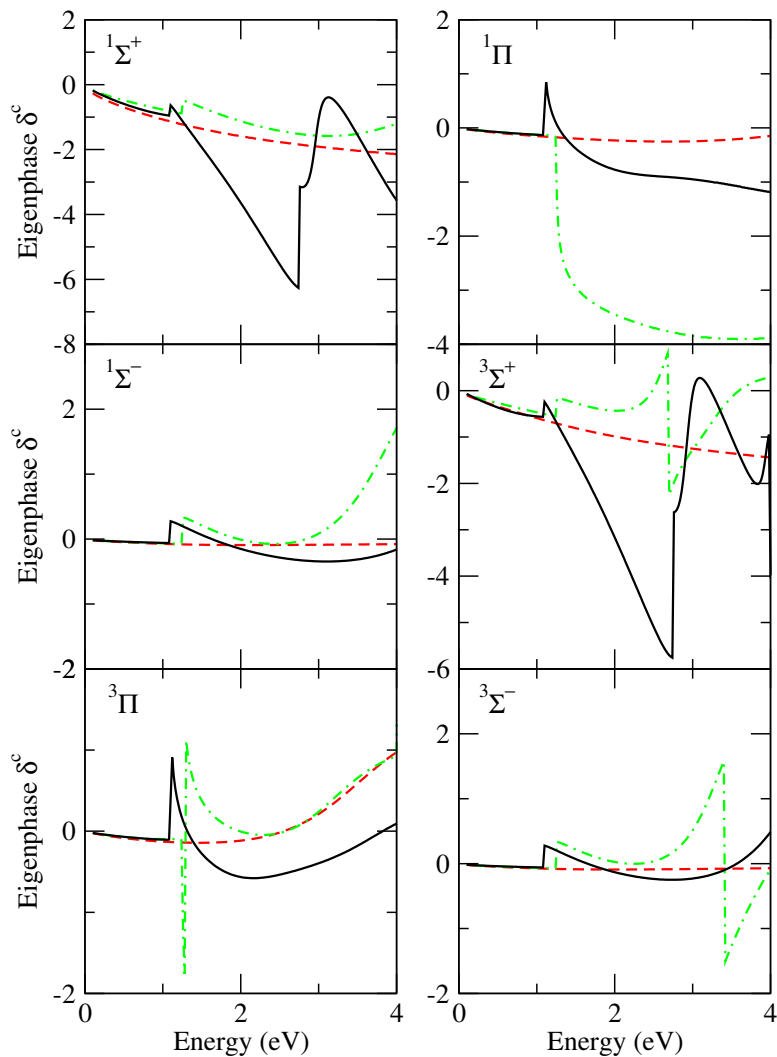
**Figure 1.** Electron – $C_2H$ eigenphase sums for different symmetries for the SCF-SE(dash), SCF-CC(dash-dot) and MRCI-CC(solid) models.

### 4.1. Target calculations

Quantemol-N was used to carry out HF and CAS-CI calculations using DZP and cc-pVDZ basis sets. Tests were performed with several other basis sets, including the ANO basis recommended by Widmark et al. (1990) for the $C_3N$ but for which we were unable to get satisfactory results.

Models 2 and 4, used a $10\sigma$, $3\pi$ orbital space, with 8 electrons frozen in the $1 - 4\sigma$ orbitals and the remaining 17 electron distributed among the $5 - 10\sigma$ and all the $\pi$ orbitals. This CAS-CI model was retained for use in model 5, which made use of MOLPRO MRCI orbitals; these NOs were obtained by the state-averaging the lowest $^2A_1$, $^2B_1$, $^2B_2$, and $^2A_2$ MRCI states in a 5:2:2:1 weighting, manually chosen in order to produce good target characteristics for the scattering run.

Table 4 compares our target models with the results of previous electronic structure calculations. $C_3N$ is a more complicated system than $C_2H$ and there is less agreement
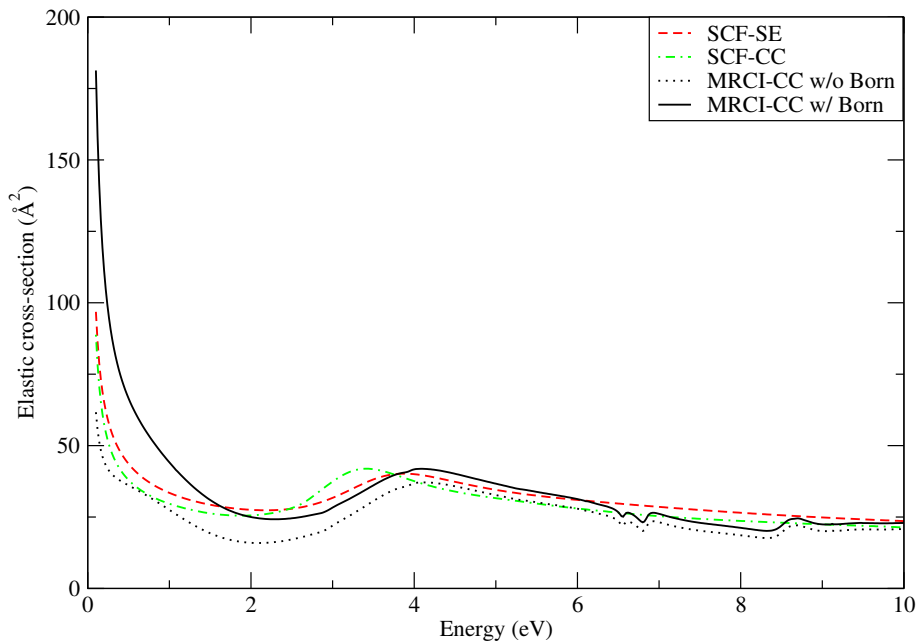
**Figure 2.** Elastic Cross-Section for electron $C_2H$ collisions

**Table 4.** Selected calculated target properties of $C_3N$. All results are for the equilibrium geometry of $C_3N$. The calculated absolute energies of the X $^2\Sigma^+$ ground state is given in Hartree while the vertical excitation energy to the low-lying A $^2\Pi$ is given in eV. $\mu$ is the ground state dipole moment, given in Debye. See text for details of models.

| Model | Basis | Orbitals | Method | X $^2\Sigma^+$ | $\mu$ | A $^2\Pi$ |
|---|---|---|---|---|---|---|
| This work/1 | DZP | SCF | HF | -167.870 | 2.332 | |
| 2 | DZP | SCF | CAS-CI | -167.933 | 1.288 | 1.038 |
| 3 | cc-pVDZ | SCF | HF | -167.871 | 2.749 | |
| 4 | cc-pVDZ | SCF | CAS-CI | -167.937 | 2.270 | 1.235 |
| 5 | cc-pVTZ | NOs | CAS-CI | -168.003 | 3.655 | 0.406 |
| Feher (1992) | 6-31G* | | UMP2 | -168.345 | 3.270 | |
| Sadlej & Roos (1991) | ANO | CAS-SCF | CAS-SCF | | 2.920 | 0.750 |
| | | CAS-SCF | MRCI | | 3.040 | 0.400 |
| McCarthy et al. (1995) | cc-pVTZ | | RCCSD(T) | -167.440 | | 0.266 |
| | cc-pVQZ | | RHF | -168.071 | 3.254 | |
| | | | RCCSD | -167.439 | 2.887 | |
| | | | RCCSD(T) | -167.400 | 2.852 | 0.270 |

between these calculations on important properties such as the lowest vertical excitation energy and the permanent target dipole moment. Despite a thorough search no experimental dipole moments could be found for the neutral molecule
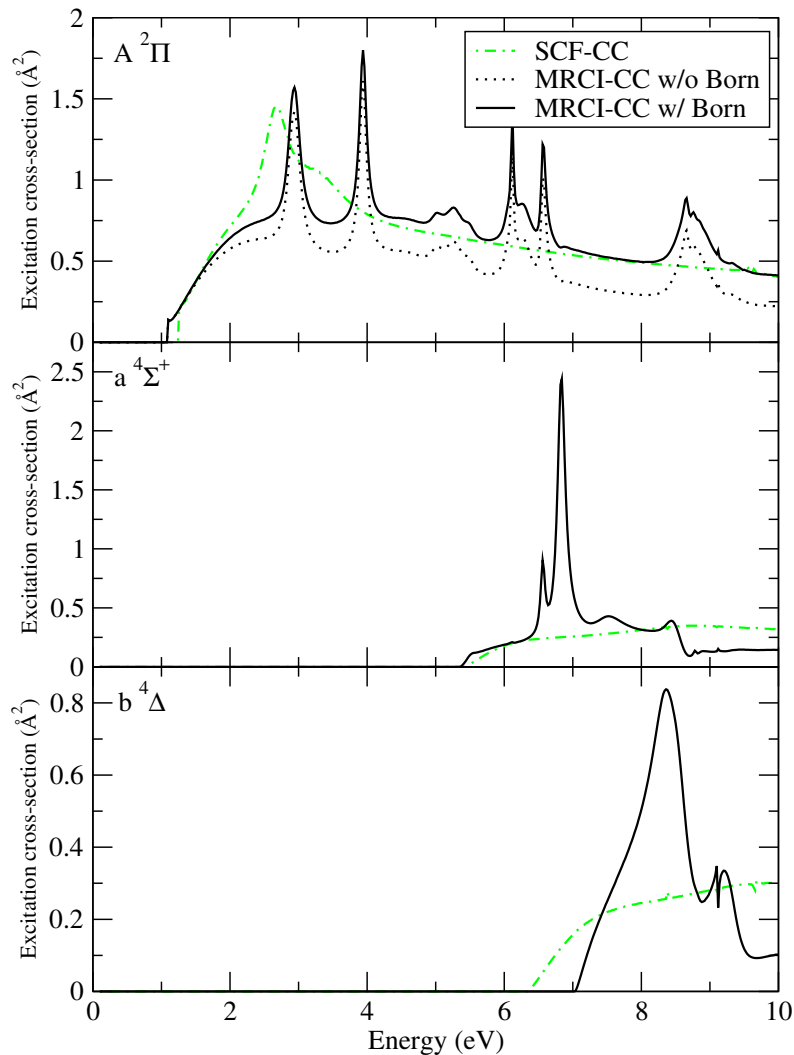
**Figure 3.** Electron impact electronic excitation cross sections for $C_2H$ final state: A $^2\Pi$, a $^4\Sigma^+$ and b $^4\Delta$.

### 4.2. Scattering calculations and bound anion states

Again a 48-state calculation was carried out (doublet and quartet states with 6 states per symmetry being included). The 40 target states below 10eV retained in the outer region. 46 in Quantemol-N jobs. As for $C_2H^-$ the bound state calculations retained only the X $^2\Sigma^+$ and A $^2\Pi$ target states, and were propagated to 30.1 $a_0$.

Table 5 presents the calculated electronic bound states for all models, as well as previous results from literature. All models find the deeply bound X $^1\Sigma^+$ state, with CC calculations finding the state between 1 and 1.5 eV deeper, furthermore use of the MRCI-CC calculation bring the bound state even deeper to about 4 eV, closer in line with data from previous results in the literature. This model also finds numerous other weakly bound states of $C_3N^-$, presented in Table 6. It should be noted that model 3 (SCF-SE calculation using the cc-pVDZ basis set) also finds the $^{1,3}\Pi$ bound state at 0.0002 eV, although this was not found in any other models that use SCF orbitals.

**Table 5.** $C_3N^-$ bound states with energies given in eV. All results are for the equilibrium geometry of $C_3N$

| Model | Basis | Orbitals | Method | X $^1\Sigma^+$ |
|---|---|---|---|---|
| This work/1 | DZP | SCF | SE | 2.793 |
| 2 | DZP | SCF | CC | 3.896 |
| 3 | cc-pVDZ | SCF | SE | 2.248 |
| 4 | cc-pVDZ | SCF | CC | 3.788 |
| 5 | cc-pVTZ | MRCI | CC | 4.009 |
| Botschwina & Oswald (2008) | VQZ+ | RHF | RHF | 3.651 |
| | VQZ+ | RHF | RCCSD | 4.343 |
| | VQZ+ | RHF | RCCSD(T) | 4.395 |
| Kolos et al. (2008) | aug-cc-pCV5Z | RHF | RHF | 3.650 |
| | aug-cc-pCV5Z | RHF | RCCSD | 4.363 |
| | aug-cc-pCV5Z | RHF | RCCSD(T) | 4.417 |
| Zhan & Iwata (1996) | 6-31G+(d) | HF | HF | 2.519 |

**Table 6.** Binding energies, in eV, of the states of $C_3N^-$ calculated for the MRCI-CC scheme (model 5).

| | Singlet | Triplet |
|---|---|---|
| $\Sigma^+$ | | 0.0012 |
| | 0.5490 | 0.5490 |
| | | 0.6241 |
| | | 0.6220 |
| | 4.0094 | 4.0094 |
| $\Pi$ | 0.0003 | 0.0003 |

There appears to be no prediction of bound states other than the X $^1\Sigma^+$ states in the literature.

### 4.3. Resonances

Figure 4 presents the eigenphase sums for $C_3N^-$ calculations. Table 7 summarizes the resonance data for $C_3N^-$ calculations, with the same method being employed as previously described for the $C_2H^-$ resonances. The SE models all find shape resonances of $^1\Pi$ and $^3\Pi$ symmetries. These appear in all CC calculations at about 0.1 eV lower in electron scattering energy, with the width remaining quite stable for the $^1\Pi$ resonance, and at about 0.2 – 0.4 eV lower scattering energy with a narrower width for the $^3\Pi$ resonance. In all CC calculations, Feshbach resonances appear in $^1\Sigma^-$, $^1\Delta$, $^3\Sigma^+$, $^3\Sigma^-$ and $^3\Delta$ symmetries. These resonances appear systematicaly at higher energies for the larger cc-pVTZ basis compared to cc-pVDZ when using SCF orbitals. However the use

**Table 7.** $C_3N^-$ low-lying resonance positions (and widths) in eV

| Model | 1 | 2 | 3 | 4 | 5 |
|---|---|---|---|---|---|
| $^1\Pi$ | 2.905 (0.471) | 2.716 (0.452) | 2.989 (0.444) | 2.822 (0.475) | 2.749 (0.437) |
| $^1\Sigma^-$ | | 2.29 a | | 2.191 (0.158) | 2.094 (0.153) |
| $^1\Delta$ | | 2.307 (0.161) | | 2.248 (0.176) | 2.167 (0.184) |
| $^3\Sigma^+$ | | 0.987 (0.016) | | 1.327 (0.023) | 0.741 (0.034) |
| $^3\Pi$ | 1.342 (0.204) | 1.167 (0.121) | 1.632 (0.220) | 1.25 a | 1.426 (0.141) |
| $^3\Sigma^-$ | | 1.705 (0.053) | | 2.163 (0.063) | 1.666 (0.075) |
| $^3\Delta$ | | | | | 0) |

$^a$ Resonan
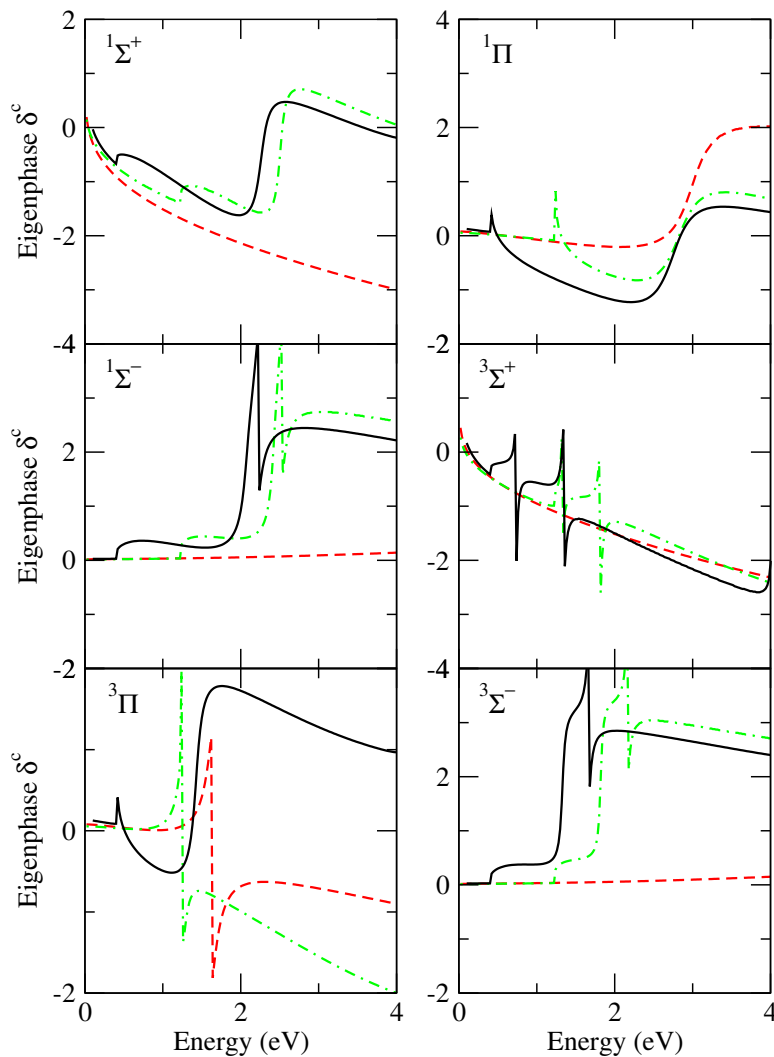


**Figure 4.** Electron – $C_3N$ eigenphase sums: for SCF-SE(dash), SCF-CC(dash-dot) and MRCI-CC(solid) models.

of MRCI NO's leads to lower resonance positions than either SCF-CC models for all symmetries. The Feshbach resonance widths remain stable across all CC models.
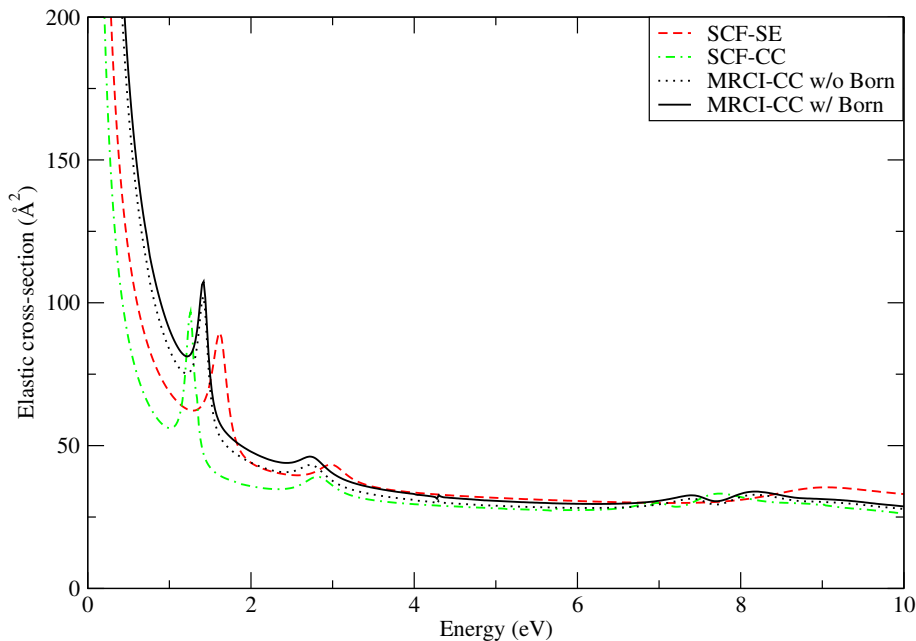
**Figure 5.** $C_3N$ Elastic Cross-Section

## *4.4. Cross-sections*

Figure 5 presents the total elastic cross-section of $C_3N$ for electron scattering energies up to 10 eV, for three models, SCF-SE, SCF-CC and MRCI-CC. Born corrected results for the MRCI-CC model are also shown.

Figures 6 shows inelastic cross-sections representing the excitation from the $^2\Sigma^+$ ground state of the neutral to the first two excited states, both of which are $^2\Pi$; the Born correction is applied to both excitations. The comparison between the SCF-CC and the MRCI-CC models shows us that the use of MRCI orbitals increases the cross-sections at all energies, although both models share similar features (such as the threshold spike in B $^2\Pi$ excitation). Again the extra resonances shown by the MRCI-CC model should be treated with caution.

## 5. Conclusions

The presence of electronic resonance features above 1 eV for both molecules suggests that formation of temporary negative ions by electrons trapped in these resonance states is an unlikely mechanism for radiative electron attachment in the ISM. This is because 1 eV converts to a much higher temperature than electrons are found at in the ISM, making it highly unlikely electrons will reach the energies required to become temporarily trapped in the resonance states.

The more likely possibility is that the molecular anions observed may be arise from the very weakly bound anionic states, as found for $C_3N^-$. These states will support nuclear excited states which lie in the continuum and therefore are resonances. We
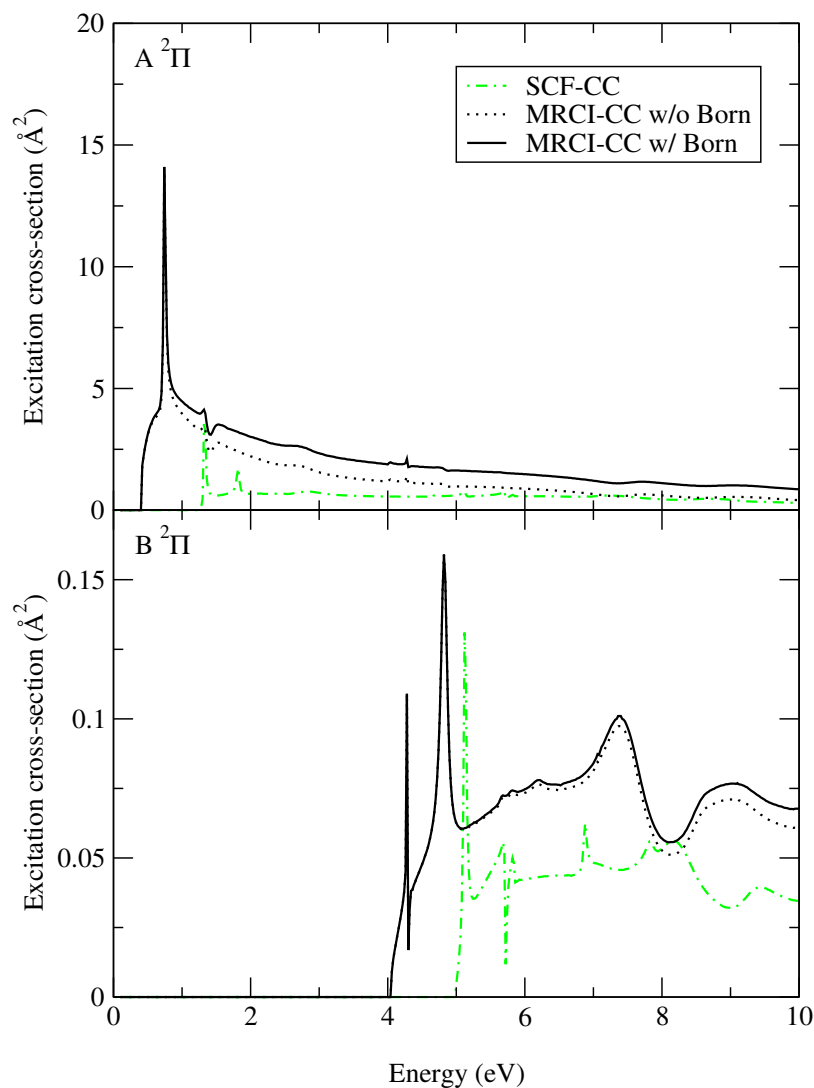
**Figure 6.** $C_3N$ electron impact electronic excitation cross sections to A $^2\Pi$ and B $^2\Pi$.

note that $C_2H^-$ appears not to support such states. If this mechanism does explain the formation of such anions, $C_3N^-$ would be observed in large quantities but $C_2H^-$ would not. This prediction appears to match current observations. We will investigate this proposal further in future work, both for the molecules in this paper, and by investigating other molecules in the $C_nN^-$ and $C_nH^-$ series.

### Acknowledgements

# References

Agundez M, Cernicharo J, Guelin M, Kahane C, Roueff E, Klos J, Aoiz F J, Lique F, Marcelino N, Goicoechea J R, Garcia M G, Gottlieb C A, McCarthy M C & Thaddeus P 2010 *Astron. Astrophys. Lett.* **517**, L2.

Baker J, Nobes R H & Radom L 1986 *J. Comp. Chem.* **7**, 349–358.

Baluja K L, Mason N J, Morgan L A & Tennyson J 2000 *J. Phys. B: At. Mol. Opt. Phys.* **33**, L677–L684.

Botschwina P & Oswald R 2008 *J. Chem. Phys.* **129**, 044305.

Brunken S, Gupta H, Gottlieb C A, McCarthy M C & Thaddeus P 2007 *Astrophys. J.* **664**, L43–L46.

Burke P G & Berrington K A, eds 1993 *Atomic and Molecular Processes, an R-matrix Approach* Institute of Physics Publishing Bristol.

Cernicharo J, Guelin M, Agundez M, McCarthy M C & Thaddeus P 2008 *Astrophys. J.* **688**, L83–L86.

Cui Q & Morokuma K 1998 *J. Chem. Phys.* **108**, 626–636.

Ervin K M & Lineberger W C 1991 *J. Chem. Phys* **95**, 1167.

Faure A, Gorfinkiel J D, Morgan L A & Tennyson J 2002 *Computer Phys. Comms.* **144**, 224–241.

Feher M 1992 *Chem. Phys. Let.* **188**, 609–612.

Fortenberry R C, King R A, Stanton J F & Crawford T D 2010 *J. Chem. Phys.* **132**.

Gupta H, Brunken S, Tamassia F, Gottlieb C A, McCarthy M C & Thaddeus P 2007 *Astrophys. J.* **655**, L58–L60.

Harada N & Herbst E 2008 *Astrophys. J.* **685**, 272–280.

Herbst E & Osamura Y 2008 *Astrophys. J.* **679**, 1670–1679.

Janousek B K, Brauman J I & Simons J 1979 *J. Chem. Phys.* **71**, 2057.

Kolos R, Gronowski M & Botschwina P 2008 *J. Chem. Phys.* **128**, 154305.

McCarthy M C, Gottlieb C A, Gupta H & Thaddeus P 2006 *Astrophys. J.* **652**, L141–L144.

McCarthy M C, Gottlieb C A, Thaddeus P, Horn M & Botschwina P 1995 *J. Chem. Phys.* **103**, 7821–7827.

Millar T J, Walsh C, Cordiner M A, Chumin R N & Herbst E 2007 *Astrophys. J.* **662**, L87–L90.

Morgan L A, Tennyson J & Gillan C J 1998 *Computer Phys. Comms.* **114**, 120–128.

Natterer J & Koch W 1995 *Molecular Physics* **84**, 691–706.

Petrie S & Herbst E 1997 *Astrophys. J.* **491**, 210–215.

Sadlej J & Roos B O 1991 *Chem. Phys. Let.* **180**, 81–87.

Sarpal B K, Branchett S E, Tennyson J & Morgan L A 1991 *J. Phys. B: At. Mol. Opt. Phys.* **24**, 3685–3699.

Taylor T R & Xu C S 1998 *J. Chem. Phys.* **108**, 10018–10026.

Tennyson J 1996 *J. Phys. B: At. Mol. Opt. Phys.* **29**, 6185–6201.

Tennyson J 2010 *Phys. Rep.* **491**, 29–76.

Tennyson J, Brown D B, Munro J J, Rozum I, Varambhia H N & Vinci N 2007 *J. Phys. Conf. Series* **86**, 012001.

Tennyson J & Noble C J 1984 *Computer Phys. Comms.* **33**, 421–424.

Terzieva R & Herbst E 2000 *International Journal of Mass Spectroscopy* **201**, 135–142.

Thaddeus P, Gottlieb C A, Gupta H, Brunken S, McCarthy M C, Agundez M, Guelin M & Cernicharo J 2008 *Astrophys. J.* **677**, 1132–1139.

Vuitton V, Lavvas P, Yelle R V, Galand M, Wellbrock A, Lewis G R, Coates A J & Wahlund J E 2009 *Planet. Space Sci.* **57**.

Werner H J, Knowles P J, Lindh R, Manby F R, Schütz M, Celani P, Korona T, Mitrushenkov A, Rauhut G, Adler T B, Amos R D, Bernhardsson A, Berning A, Cooper D L, Deegan M J O, Dobbyn A J, Eckert F, Goll E, Hampel C, Hetzer G, Hrenar T, Knizia G, Köppl C, Liu Y, Lloyd A W, Mata R A, May A J, McNicholas S J, Meyer W, Mura M E, Nicklass A, Palmieri P, Pflüger K, Pitzer R, Reiher M, Schumann U, Stoll H, Stone A J, Tarroni R, Thorsteinsson T, Wang M & Wolf A 2008 'Molpro, version 2008.3, a package of ab initio programs'. see http://www.molpro.net.

Widmark P O, Malmqvist P A & Roos B O 1990 *Theor Chim Acta* **77**, 291–306.

Woon D E 1995 *Chem. Phys. Let.* **244**, 45 – 52.

Zhan C G & Iwata S 1996 *J. Chem. Phys.* **104**, 9058–9064.